J. Int. Environmental Application & Science, Vol. 4 (1): 1-21 (2009)

Influence of Inlet Conditions and Burner Tripping on NO and Temperature Characteristics in a Tangentially Fired Furnace

R. Ben-Mansour, M. A. Habib*, H. I. Abualhamayel

Mechanical Engineering Department, King Fahd University of Petroleum & Minerals, Dhahran 31261, Saudi Arabia

Received August 25, 2008; Accepted February 06, 2009

Abstract: Tangentially-fired furnaces have been used successfully and extensively throughout the world with many types of oils, gas and coal as fuels and are widely used in steam generators of thermal power plants. The present study provides the NO and temperature distributions in the combustion chamber and in the exhaust gas at various operating conditions of excess air factor with varying the air mass flow rate, combustion air temperature and the number of tripped burners. In particular, the simulation provided correlations for NO concentration and each of the maximum furnace temperature and furnace average temperatures. The results show that the temperature distributions are significantly distorted by tripping any of the burners. The results also show that tripping one or two burners either adjacent or opposite or tripping four burners results in regions of high temperature gases close to the walls. The results have shown that the furnace average temperature and NO concentration decrease as the excess air factor increases for a given air mass flow rate. As the combustion air temperature increases, furnace temperature increases and the thermal NO concentration increases sharply. Heat absorptions in super heater and economizer are greatly influenced by combustion air temperature and excess air factor and are slightly influenced by burner tripping. Correlations were obtained for the influence of the combustion air temperature and air to fuel ratio on NO maximum values and NO values at outlet section.

***Key words**: Tangentially fired furnace; Burner Tripping; NO Characteristics; Temperature Characteristics*

Introduction

NO formation during the combustion process in gas-fired boilers occurs mainly through the oxidation of nitrogen in the combustion air by two mechanisms known as thermal NO and prompts NO. The rate of thermal NO formation is directly affected by the combustion zone temperature and the oxygen concentration. The formation of NO in tangentially fired boilers is a very complicated problem due to many parameters that influence its formation process. These parameters include fuel to air ratio, inlet air temperature as well as the number of tripped burners. Prediction and empirical modelling (Robinson, 1985) show the expected vortex in the middle of the furnace and recirculation zones near the bottom and side walls. A high turbulence level at any point in the flow field results in relatively larger fluctuation of the local reaction rates. Complex 3D models for equipment design and operational changes are usually based on computational Fluid Dynamics CFD (Li & Thompson, 1996). Due to the expensive price of measurements of the combustion characteristics and the limitation by the geometry, time and the number of instruments and skills required, only a few detailed works on large capacity boilers are reported in the literature (Van der Lans *et al.,* 1998; Xiang *et al*., 2000; Liierup *et al*., 1994; Walsh et al., 1994). The use of computational fluid dynamics (CFD) codes for modelling utility boilers is becoming a useful tool to predict the performance of utility boilers and the NO emission (Fan *et al*., 1999), which has the potential to become an important design tool to help the engineers to optimize the operating conditions, reduce pollution emission, improve the design of new boilers and evaluate the retrofit of the old boilers. Coelho and Carvalho (1996) established a three-dimensional numerical model to predict the temperature and

**Corresponding: E-mail: mahabib@kfupm.edu.sa; Tel:00 966 3 860 4467; Fax:00 966 3 860 2949*

species concentration in a power station boiler. They solved the governing momentum, energy and species equations and compared their results with experimental data measured and found that there is a good agreement between the computed and measured results although the temperature was under-predicted, especially in the burner region. Moreover, this comparison indicated that the combustion model based on chemical equilibrium assumption results in a better prediction of the species concentrations.

A one-component model to represent oil- and gas-fired boilers was developed and implemented in a system simulation program by Handby and Li (1997). The objective of their study was to calculate the emissions of NO, CO and SO_x, in addition to prediction of the performance of the boiler. It was found that NO formation could be calculated satisfactorily from established chemical rate equations in the case of gas-fired units, with separate consideration of the prompt and thermal routes. The application of a full three-dimensional mathematical model to a fuel-oil fired power station boiler was conducted by Coelho and Carvalho (1995). Several variants of thermal and fuel-NO formation models were applied to the prediction of NO concentration in a utility boiler. Models for thermal and fuel-NO formation were included and several variants of the models were employed. The NO mole fraction was significantly under-predicted. It was shown that the role of fuel-NO and the super-equilibrium of oxygen atom concentration are not responsible for the differences observed. The most probable reasons for the discrepancies were attributed to the errors in the temperature prediction and in the measurements.

Cold modelling test was performed for tangentially fired boiler by Zhou et al (1999). The effect of furnace arch structure and furnace height on velocity deviation of flue-gas channel was studied. Cold modelling test was performed by Zhou et al (1999) to study flow field in furnace and horizontal flue gas channel under normal condition and those of counter-tangent stream for tangentially fired boiler. Based on the cold modelling test on a tangentially fired boiler, the cold flow field in furnace and the velocity deviation in the horizontal flue gas pass were numerically investigated by Thou et al (2001). The flow characteristics in furnace and the forming mechanism of the flue gas velocity deviation were analyzed, and the measures to decrease the flue gas velocity deviation were recommended. CFD models are founded on fundamental physical principles and can thus predict fluid flow and heat transfer properties within boilers and under specific operational conditions. Submodels such as combustion, turbulence, and NO formation can be added as subroutines (Dong 2000). The mechanisms of NO formation and correlations can be captured by mathematical models (Li, 1997, Li & Thompson, 1996; Dong, 2000). Most of the previous work was conducted on tangentially fired furnaces on coal combustion (Liu *et al*., 2001; Zheng *et al*., 2000; Chen *et al*., 1992; Yin *et al*., 2002; Fan *et al*., 2001a,b; Boyd *et al*., 1985; Chong *et al*., 2001; Mathur *et al*., 2001; Luis *et al*., 2005; Lou & Zhou, 2005; Zhou *et al*., 2004; Afonso *et al*., 1993).

Zheng *et al*. (2000) presented numerical and experimental study on reduction of NO emissions in the furnace of a tangentially fired boiler under different operating conditions. A simplified NO formation mechanism model, along with the gas-particle multiphase flow model, was adopted. The prediction yielded encouraging results as compared to experimental data. Kokkinos *et al*. (2000, 2001) applied some techniques for reducing NO emissions from tangentially fired boilers. They applied staged combustion along the combustors front and rear walls through rerouting the location of some fuel and oxidant feed ports. The reduction of NO was achieved by installing over-fire ports equipped with air flow dampers, increasing separation between the auxiliary air and fuel nozzles during the early stage of combustion in addition to the reduction of secondary air flow through air nozzles keeping proper mixing of air and fuel under staged conditions. They also used a numerical approach to optimize the design to minimize NO emissions and reported a decrease of 50% from baseline levels. Other studies (Coelho & Carvalho, 1996; Yin *et al*., 2002) have involved the total flow and energy modelling of industrial gas furnaces. The focus in these studies was on improving the efficiency of furnaces and reducing NO pollution among other considerations. Measurements of the stability limits and temperature contour maps of flame inside a water-cooled tangentially-fired model furnace were performed by Habib *et al.* (1992, 2005). The limits of ignition were found to depend on the inclination angle of the burners and on the temperature levels.

Ma *et al*. (1999) developed a model to simulate a confined, turbulent natural gas diffusion flame model in a cylindrical combustion chamber using both eddy dissipation and non-equilibrium, mixedness-reactedness flamelet models. Turbulence was represented by a Reynolds stress model based on the

differential transport equations for stresses. Comparisons with measurements indicated that the latter model was in good agreement with measured values. On the other hand, they reported that eddy dissipation model failed to capture measured trends in the near-burner region. Actually it over predicts the temperature and under predicts the oxygen concentration since it cannot represent the turbulence-chemistry interactions and non-equilibrium effects. Hjertager *et al*. (2000, 2001) presented various turbulent combustion models in a tube including the eddy-dissipation model (EDC), the scalar mixing/dissipation theory, multiple time scale turbulent mixer models (MTS) and two presumed probability dissipation function (PDF) models. These models were compared with experimental data. They reported that the standard EDC can not predict the reaction-zone length while the MTS, EDC-MTS model gave better results including the effect of increasing Reynolds number. PDF models predicted too short reaction zone length. Yaga *et al*. (2000) developed a three-dimensional large eddy simulation turbulent combustion model (EDC) to study turbulent combustion characteristics in a co-axial combustor including the swirling effect. They compared the results of the model with experimental data for burning CH_4 and reported that temperature and CH_4 mole fraction were predicted accurately. However, due to the use of simple CO reaction mechanism, the calculated results of CO mole fraction did not agree well with experimental data.

The SIMPLEC algorithm with the power-law scheme and the pseudo-time-step method were employed to numerically solve the governing equations for 3-D turbulent flow field in a 2023 t/h rated boiler furnace using two grid systems was presented by He *et al* (2004). The calculated velocity distribution qualitatively agreed with the experimental data. As a special topic, the gas temperature deviation in large scale tangentially fired boilers was studied (Xu *et al* 2001). Gas temperature deviations were compared with the measured values in a 600 MW boiler, and an approximate agreement between calculations and measurements was found. It was concluded that residual airflow swirling and platen super-heaters were the two important causes for the gas temperature deviation. Determination of NO emissions from strong swirling confined flames with an integrated CFD-based procedure was conducted by Frassoldati *et al* (2005). The model used very detailed and comprehensive reaction schemes on the basis of the results obtained from CFD computations. The procedure was validated in the case of high swirled confined natural gas diffusion flames.

Backreedya *et al* (2005) considered two approaches that can be employed for prediction of NO and unburned carbon. The first approach uses global models such as the 'slice' model which requires the combustor reaction conditions as an input but which has a detailed coal combustion mechanism. The second involves a computational fluid dynamic model that in principle can give detailed information about all aspects of combustion, but usually is restricted in the detail of the combustion model because of the heavy computational demands. Some of the combustion properties can be predicted by means of empirical correlations but these tests can be unsuccessful when applied to predict combustion behaviour such as ignition and NO emissions. Computational fluid dynamics based retrofits to reheater panel overheating of a power plant was utilized by He *et al* (2007) to numerically diagnose the metal surface overheating issues of the reheater pendants that exist in the full-scale boiler of Power Station in China. The basic conclusion was that some corresponding measures must be taken to rebuild the flow field constructions in order to effectively avoid the boiler reheater and superheater pendant metal overheatings.

In the present work, calculation of the flow field, and temperature and NO concentration-contour maps in a tangentially-fired furnace are provided. The investigation covers a range of different parameters such as the number of tripped burners, air to fuel ratio and combustion air temperature. The details of the flow, thermal and NO fields are obtained from the solution of the conservation equations of mass, momentum and energy and transport equations for scalar variables in addition to the equations of the turbulence model. Available experimental measurements are used for validating the calculation procedure.

Boiler description

The boiler considered in the present study is 1699 MW, gas fired with natural gas, water-tube boiler, having four level of burners; each level has eight burners. The boiler is composed of a furnace

(radiation section) and return tube bank (convection section). The boiler is used for production of electrical power. The steam flow rate is 1290 t/h. Steam pressure and steam temperature are 137 bar and 512^{o}C. The combustion chamber has a cross section of 26 x 10.4 and a height of 29.6 m length. A schematic of the boiler is shown in Figure1. The furnace has 32 burners distributed in 4 levels. The burners are located at elevation of 14.421, 16.041, 17.661 and 18.281 m above the furnace bottom surface. Each elevation has 8 burners. Eight burners are located at the corners of the furnace each with an inclination angle of θ; which is defined as the angle between the burner axis and the furnace diagonal. The furnace cross section is shown in the figure.

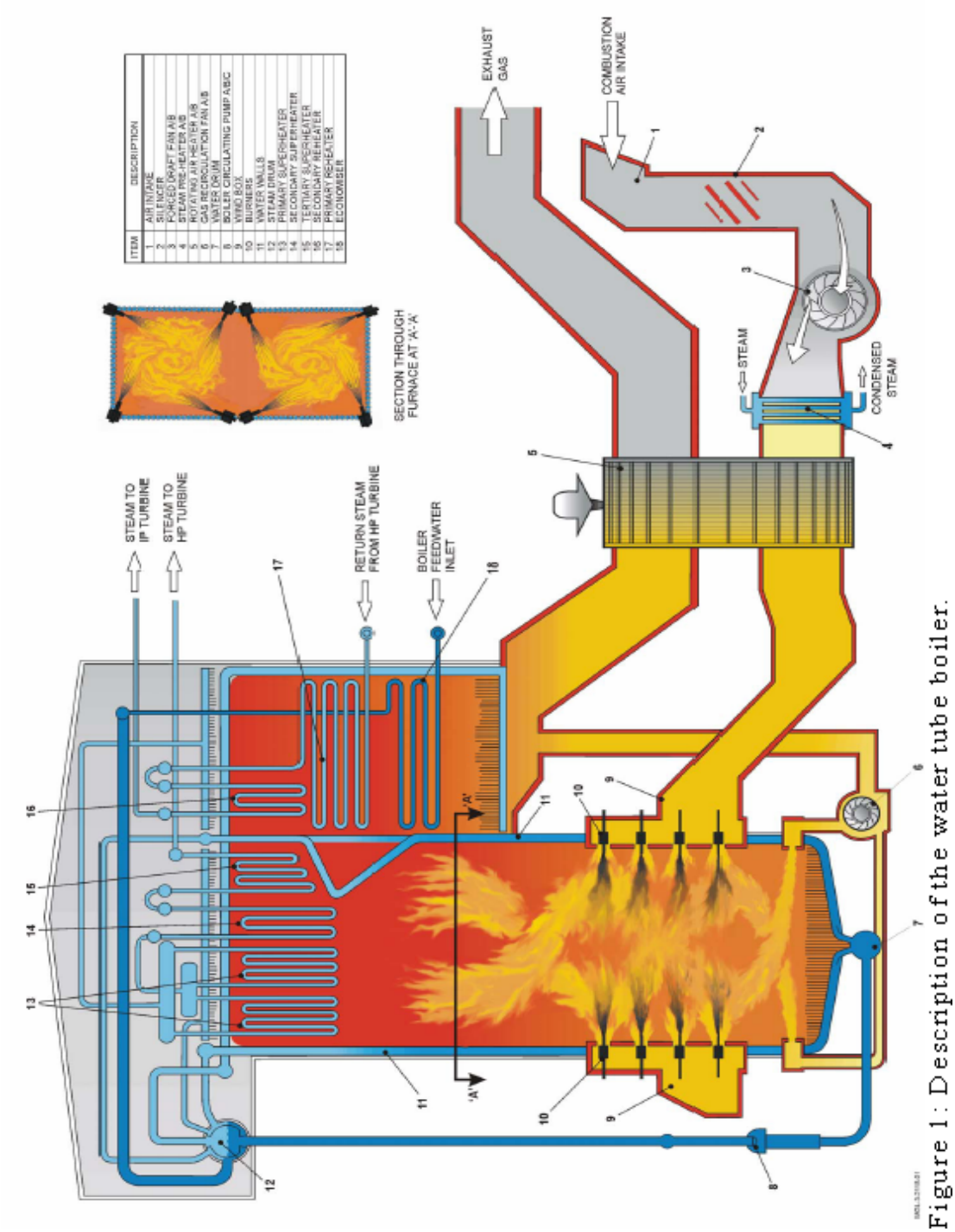

Figure 1: Description of the water tube boiler.

Mathematical formulation

The mathematical model is based on the numerical solution of the conservation equations for mass, momentum, and energy, and transport equations for scalar variables. The equations, which are elliptic and three-dimensional, are solved to provide predictions of the flow pattern, thermal and pollution characteristics of reacting flows inside a model of a tangentially fired furnace. The governing equations, turbulence and combustion models as well as the boundary conditions and the solution procedure are presented in the following.

The governing equations

The equations which govern the conservation of mass, momentum and energy as well as the equations for species transport may be expressed in the following general form (Reynolds, 1987; Shih et al, 1995):

$$\frac{\partial}{\partial x_j}\left(\bar{\rho}\,\bar{U}_j\Phi + \bar{\rho}\,\overline{u_j\phi}\right) = \frac{\partial}{\partial x_j}[\Gamma_\phi \frac{\partial \Phi}{\partial x_j}] + \bar{\rho}\,S_\Phi \qquad (1)$$

Where Φ is the dependent variable and u_j is the velocity component along the coordinate direction x_j. $\bar{\rho}$ is the fluid density; Γ_Φ is the diffusion coefficient and S_Φ is the source term.

Equation (1) stands for the mass conservation equation when Φ = 1; the momentum conservation equation when Φ is a velocity component; the energy equation when Φ is the stagnation enthalpy; or the transport equation of a scalar when Φ is a scalar variable such as mixture fraction. The present work utilizes the K-ε model of Versteeg and Malalasekera (1995). The Reynolds stresses and turbulent scalar fluxes in the model are related to the gradients of the mean velocities and scalar variable, respectively, via exchange coefficients as follows (Versteeg & Malalasekera, 1995):

$$-\rho\overline{u_i u_j} = \mu_t\left(\frac{\partial \bar{U}_i}{\partial x_j} + \frac{\partial \bar{U}_j}{\partial x_i}\right) - \frac{2}{3}\rho k\delta_{ij} \qquad (2)$$

$$-\rho\overline{u_j\phi} = \Gamma_\Phi \frac{\partial \Phi}{\partial x_j} \qquad (3)$$

Where μ_t is the turbulent viscosity and Γ_Φ is equal to μ_t / σ_Φ. The turbulent viscosity is modelled as

$$\mu_t = c_\mu\, \rho\, f_\mu K^2/\varepsilon \qquad (4)$$

Where c_μ and f_μ and σ_Φ are constants. The turbulent viscosity is thus obtained from the solution of the transport equations for K and ε. RNG (Renormalized group) turbulence model, Wilcox (2000), was used to provide better results for vortex flows. The eddy dissipation model utilizing turbulence-chemistry interaction (Magnussen & Hjertager 1976) was utilized in the present work to provide the reaction rate of production of species. In order to correctly predict the temperature distribution in the furnace a radiative transfer equation (RTE) for an absorbing, emitting and scattering medium was solved. Once the radiative intensity is obtained, the gradient of the radiative heat flux vector was found and substituted into the enthalpy equation to account for heat sources (or sinks) due to radiation. The solution of the RTE for this application was obtained using the discrete ordinates (DO) radiation model (Raithby & Chui, 1990). The blackbody spectral emissive power is calculated through using variables by Liu et al. (1998) and Zheng et al (2000) based on expressions of Modak (1979) and Smith *et al* (1982).

Conservation equations for the turbulence model

The conservation equations of the turbulence model (Reynolds, 1987; Shih et al., 1995) are given as follows:

The kinetic energy of turbulence:

$$\frac{\partial}{\partial x_j}\left(\rho \overline{U}_j k\right) = \frac{\partial}{\partial x_j}\left(\frac{\mu_{eff}}{\sigma_k}\frac{\partial k}{\partial x_i}\right) + G_k - \rho\varepsilon \tag{5}$$

The rate of dissipation of the kinetic energy of turbulence:

$$\frac{\partial}{\partial x_j}\left(\rho \overline{U}_j \varepsilon\right) = \frac{\partial}{\partial x_i}\left(\frac{\mu_{eff}}{\sigma_\varepsilon}\frac{\partial \varepsilon}{\partial x_i}\right) + C_1 G_k \frac{\varepsilon}{k} - C_2^* \rho \frac{\varepsilon^2}{k} \tag{6}$$

Where G_k represents the generation of turbulent kinetic energy due to the mean velocity gradients and is given by

$$G_k = -\rho\, \overline{u_i u_j}\, \frac{\partial \overline{U}_j}{\partial x_i} \tag{7}$$

The quantities σ_k and σ_ε are the effective Prandtl numbers for k and ε, respectively and C^*_2 is given by Shih et al. (1995) as

$$C^*_2 = C_2 + C_3 \tag{8}$$

Where C_3 is a function of the term k/ε and, therefore, the model is responsive to the effects of rapid strain and streamline curvature and is suitable for the present calculations. The model constants C_1 and C_2 have the values; C_1=1.42 and C_2 =1.68. The wall functions establish the link between the field variables at the near-wall cells and the corresponding quantities at the wall. These are based on the assumptions introduced by Launder and Spalding (1974) and have been most widely used for industrial flow modelling. The details of the wall functions are provided by the law-of-the-wall for the mean velocity as given by Habib *et al*. (1982, 1989).

Species transport equations

The local mass fraction of each species m_l, is predicted through the solution of a convection-diffusion equation for the l^{th} species. The conservation equation can be expressed in the following form:

$$\frac{\partial}{\partial x_i}(\rho \overline{U}_i\, m_l) = -\frac{\partial}{\partial x_i} J_{l,i} + R_l \tag{9}$$

Where R_l is the mass rate of creation or depletion by chemical reaction of the species l $J_{l,i}$ is the diffusion flux of species l, which arises due to concentration gradients which is given by:

$$J_{l,i} = -(\rho D_{l,m} + \frac{\mu_t}{Sc_t})\frac{\partial m_l}{\partial x_i} \tag{10}$$

Where $D_{l,m}$ is the diffusion coefficient for species l in the mixture and Sc_t is the turbulent Schmidt number, $\frac{\mu_t}{\rho D_t}$ is equal to 0.7.

An eddy-dissipation model (Magnussen & Hjertager 1976) that relates the rate of reaction to the rate of dissipation of the reactant- and product-containing eddies is used to calculate the rate of reaction.

Boundary conditions

The velocity distribution is considered uniform at the inlet section with the velocity in the direction of the burner nozzle axis. Kinetic energy and its dissipation rate are assigned through a specified value of $\sqrt{K/\overline{U}^2}$ equal to 0.1 and a length scale, L, equal to the characteristic length of the inlet pipe/annulus. At the wall boundaries, all velocity components are set to zero in accordance with the no-slip conditions. Kinetic energy of turbulence and its dissipation rate are determined from the equations of the turbulence model. Constant wall temperature corresponding to saturated water temperature in tube wall of the actual boilers was considered. The production of kinetic energy and its dissipation rate at the wall-adjacent cells are computed on the basis of the local equilibrium hypothesis. Under this assumption, the production of k and its dissipation rate are assumed to be equal in the wall-adjacent control volume. The ε equation is not solved at the wall-adjacent cells. Thus, the production of k at the node close to the wall is taken proportional to the square of the wall shear stress. The rate of dissipation, ε, at the node close to the wall is taken proportional to $k^{3/2}$ (Versteeg & Malalasekera, 1995):

Governing Equations for NO Transport

The combustion process considered in the present study has two opportunities for NO formation. The first is the thermal NO which is controlled by the nitrogen and oxygen molar concentrations and the temperature of combustion. The second is the prompt NO which is formed from molecular nitrogen in the air combining with fuel in fuel-rich conditions. This nitrogen then oxidizes along with the fuel and becomes NO during combustion. The mass transport equation for the NO species, including convection, diffusion, production and consumption of NO was solved. To consider the effect of residence time in NO mechanisms, a Lagrangian reference frame concept (Fluent 6.2 User's Guide, 2003) is included through the convection terms in the governing equations written in the Eulerian reference frame. The principal reactions governing the formation of thermal NO are given as follows:

Formation of thermal NO

The formation of thermal NO is determined by a set of highly temperature-dependent chemical reactions known as the extended Zeldovich mechanism. The principal reactions governing the formation of thermal NO from molecular nitrogen are as follows:

$$O + N_2 \Leftrightarrow_{k-1}^{k1} N + NO \tag{11}$$

$$O_2 + N \Leftrightarrow_{k-2}^{k2} O + NO \tag{12}$$

For thermal NO, the NO species transport equation is given by:

$$\frac{\partial}{\partial x_j}\left(\rho U_j Y_{NO}\right) = \frac{\partial}{\partial x_j}[\Gamma_{NO}\frac{\partial Y_{NO}}{\partial x_j}] + \mathrm{S}_{NO} \tag{13}$$

The NO source term due to thermal NO mechanisms

$$S_{NO,thermal} = M_{NO}\frac{d(NO)}{dt} \tag{14}$$

where Y_{NO} is the mass fraction of NO in the gas phase. The NO source term due to thermal NO mechanisms is given by

$$S_{NO,thermal} = M_{NO} \frac{d(NO)}{dt} \quad (15)$$

where M_{NO} is the molecular weight of NO, and $\frac{d(NO)}{dt}$ is computed from the following equation:

$$\frac{d(NO)}{dt} = \frac{2[O](k_1 k_2 [O_2][N_2] - k_{-1} k_{-2} [NO]^2)}{k_2 [O_2] + k_{-1} [NO]} \quad (16)$$

The concentration [O] is given by the partial equilibrium [O] approach as

$$[O] = 36.64 T^{0.5} [O_2]^{0.5} \exp(-27123/T) \quad (17)$$

Where all the concentrations are having the units of mol/m^3

The expressions for the rate coefficients (m^3/(mol s) used in the NO model are given below, Hanson and Salimian (1984).

$$k_1 = 1.8 \, x 10^8 \exp(-38370/T) \quad (18)$$

$$k_{-1} = 3.8 \, x 10^7 \exp(-425/T) \quad (19)$$

$$k_2 = 1.8 \, x 10^4 \, T \exp(-4680/T) \quad (20)$$

$$k_{-2} = 3.8 \, x 10^3 \, T \exp(-20820/T) \quad (21)$$

The solution procedure

The set of governing differential equations together with the boundary conditions were solved numerically by an iterative procedure (Patankar 1980). The details of the calculation procedure can be found in previous work such as Habib and Whitelaw (1982), Attya and Habib (1990), Shuja and Habib (1996) and Habib *et al*. (1989). The CFD Fluent package was used to perform the present calculations. A mesh of more than 1,000,000 finite volumes was used and the solution was converged when the summation of the residual in the governing equation summed at all the domain nodes was less than 0.01%. The solution procedure first solves the partial differential equations for conservation of mass, momentum, and energy and combustion species. Then, the transport equation for species NO is solved to provide the NO distributions. The results are obtained for three equivalence ratio of 0.952, 0.87 and 0.8.

Results and Analysis

Validation

The experimental data of Yaga *et al* (2000) was used to validate the computational procedure. The experimental data Yaga *et al* (2000) were obtained for the combustion process inside furnace of diameter of D = 0.2 m and 0.8 length. Methane gas at a flow rate of 0.2 Nm^3/h was burned with air at a rate of 1.9 Nm^3/h at stoichiometric equivalence ratio. The fuel was introduced through a circular pipe of 5mm and the air annulus pipe has an outside diameter of 23 mm. Radial distributions of temperature and methane mole fractions were presented at a axial location of x=0.05 D. The comparisons of the calculated and measured data are shown in Figs. 2 and 3. The calculated results of Yaga *et al* (2000) using large scale eddy simulation are also presented on the same figures. The radial temperature distributions, Fig. 2 indicates that the temperature is under-predicted at the centreline and good agreement is shown in other regions. Figure 3 indicates that the mole fraction of the methane fuel is well predicted by the numerical procedure. The centreline value is under-predicted by the present calculations.

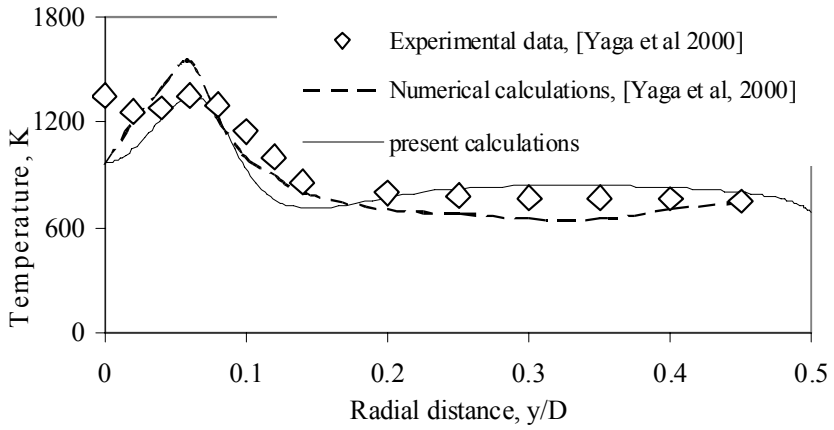

Figure 2. Comparison of calculated and measured temperature distributions at an axial location of 0.05 D

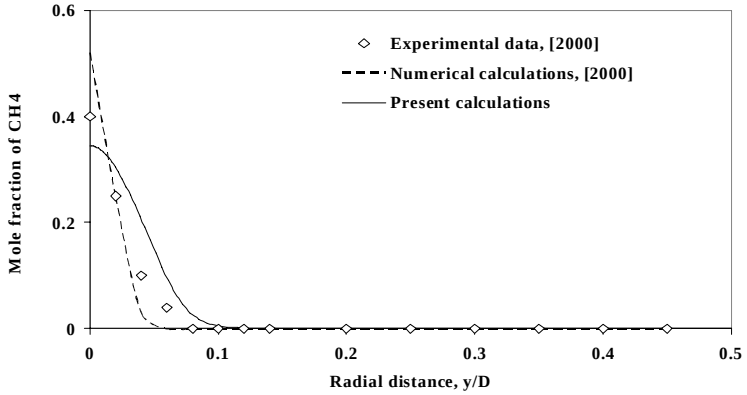

Figure 3. Comparison of calculated and measured radial distributions of mole fraction of CH_4 at an axial location of 0.05D.

Results

A set of numerical cases were considered in the present study. These refer to influence of combustion air temperature, air to fuel ratios and number of tripped burners. The basic case has a fuel flow rate of 14.29 kg/s and mass flow rate of air of 282.2 kg/s with combustion air temperature of 400 K and excess air factor pf 1.15.

Influence of combustion air temperature

The influence of the combustion air temperature is shown in Fig. 4. The combustion air temperature ranged from 400 to 600 K. The influence on the temperature contours is not significant except in the regions in the vicinity of the burners. The influence of combustion air temperature on the distribution of NO concentration is shown in Fig. 5 and indicates sharp increase in the maximum value of NO which changes from 450 at T_{air}= 400 K to 850 at T_{air}= 600 K. At the exit section, the temperature changes from around 300 K at T_{air}= 400 to 430 K at T_{air}= 500 to 670 K at T_{air}= 600 K. It is clear that the production of NO is limited to the furnace region. This is not the case downstream of the furnace region where the temperature drops to below 1400 K and NO production is insignificant. The influence of the combustion air temperature on the temperature and NO distributions across the burners' plane at levels 1 and 4 are shown in Figs. 6-9. It is clear that the temperature levels in the middle of the vortex increase by around 400 to 600 K as a result of increase in the combustion air temperature. Corresponding to increase in the temperature, the maximum levels of NO increase from 500 to 750 to 1100 ppm as the combustion air temperature increases from 400 to 500 to 600 K at burners' levels 1 and 4.

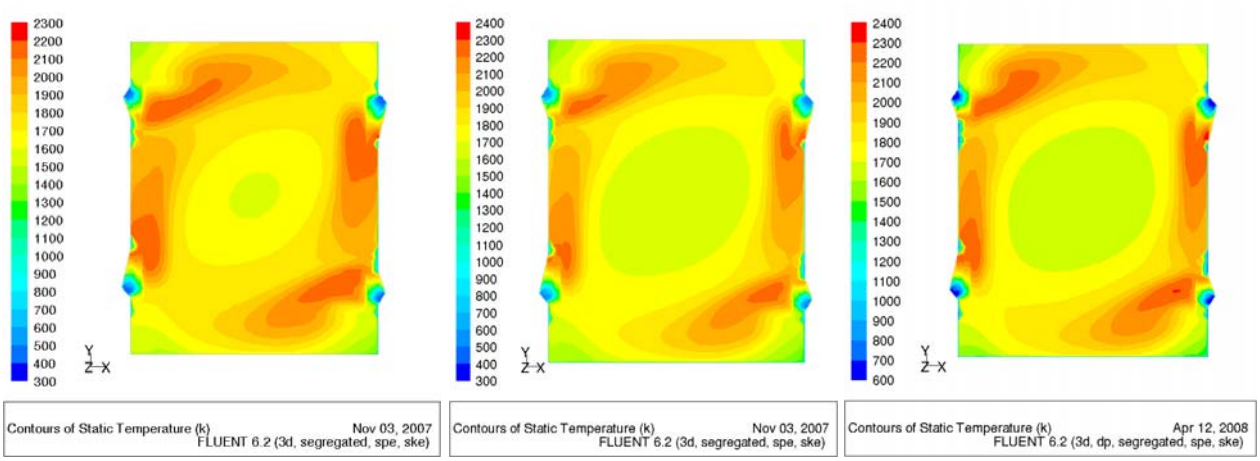

T_{air} =400 K T_{air} =500 K T_{air} = 600 K

Figure 4. Influence of combustion air temperature on temperature distribution

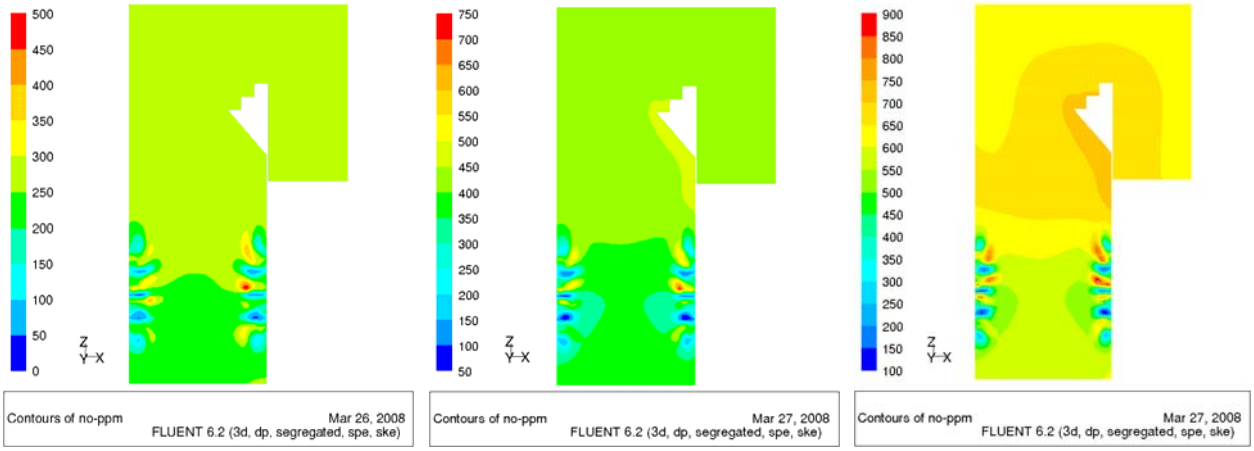

T_{air} =400 K T_{air} =500 K T_{air} = 600 K

Figure 5. Influence of combustion air temperature on NO distribution

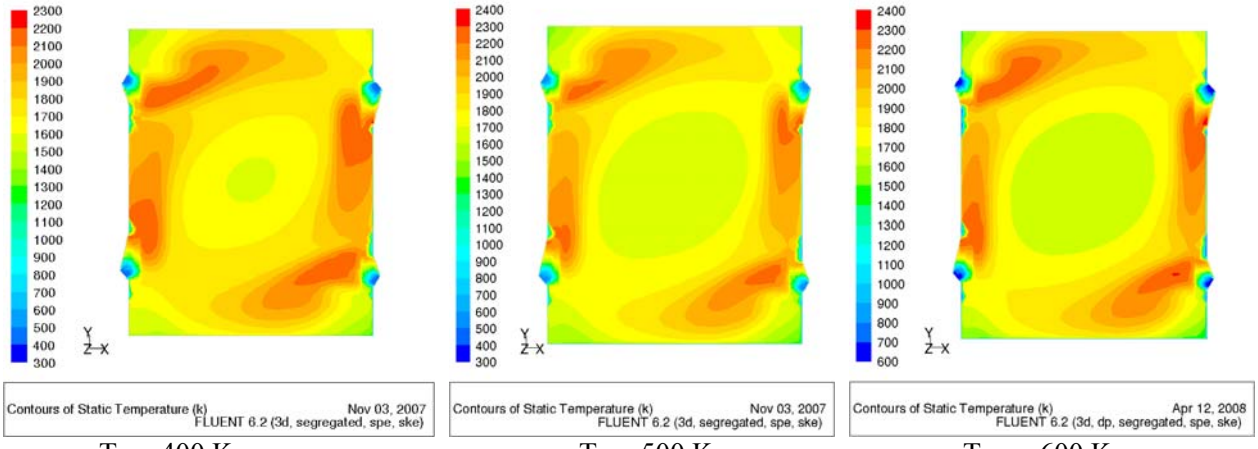

T_{air} =400 K T_{air} =500 K T_{air} = 600 K

Figure 6. Influence of combustion air temperature on temperature distribution at lower level

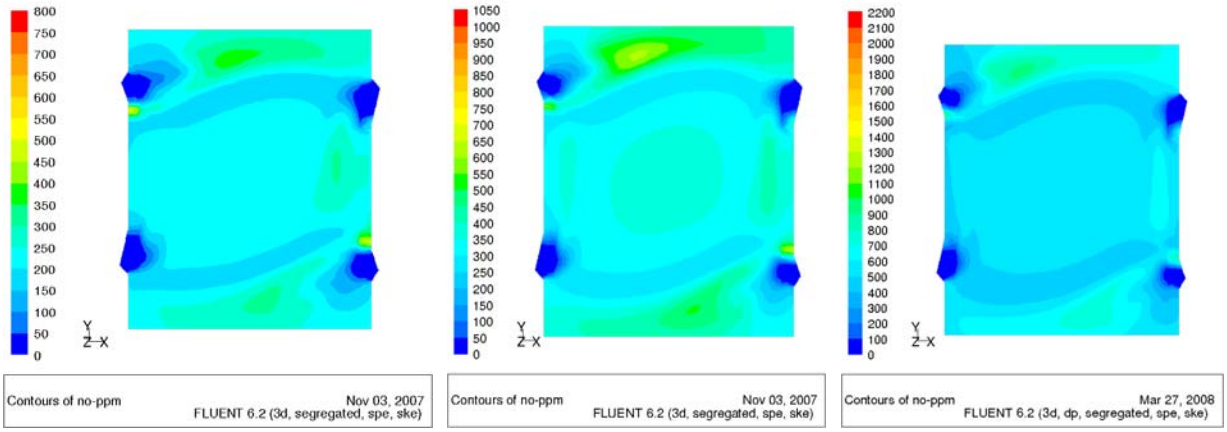

T_{air} =400 K T_{air} =500 K T_{air} =600 K

Figure 7. Influence of combustion air temperature on NO distribution at lower level

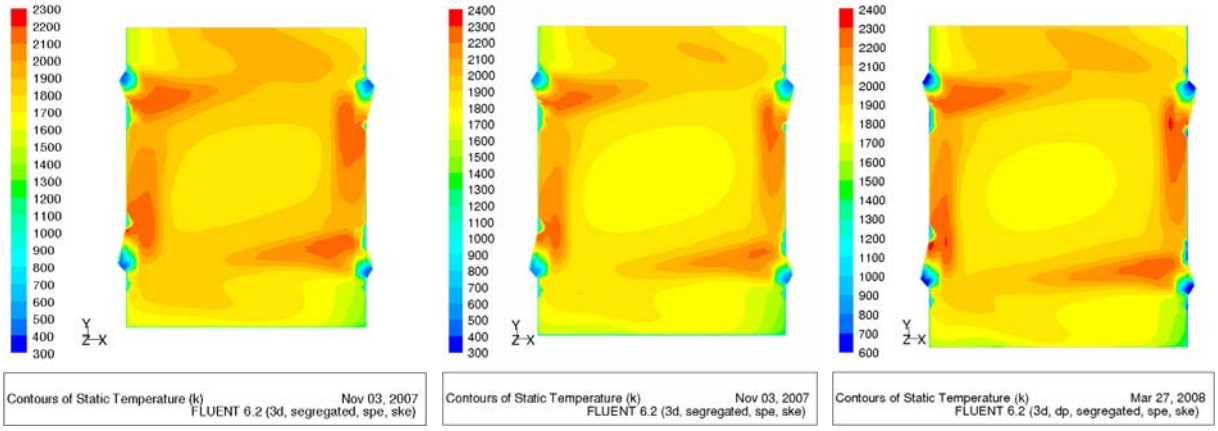

T_{air} =400 K T_{air} =500 K T_{air} =600 K

Figure 8. Influence of combustion air temperature on temperature distribution at higher level

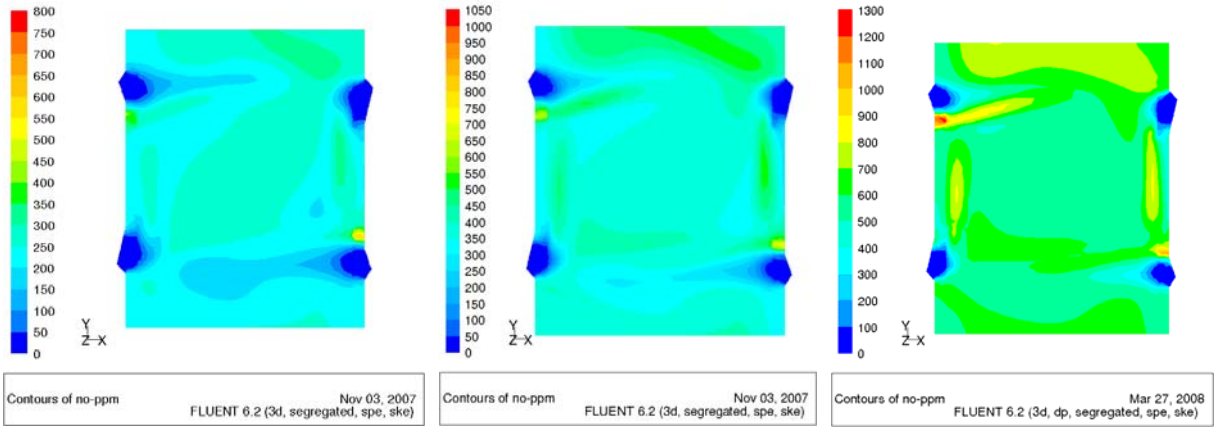

T_{air} =400 K T_{air} =500 K T_{air} =600 K

Figure 9. Influence of combustion air temperature on NO distribution at higher level

Influence of Air-to-fuel ratio

In order to investigate the influence of the air to fuel ratio on the flow temperature fields, three values of A/F ratios were considered. These are presented by excess air factors of 1.05, 1.15 and 1.25. In

this case, the vortex angle was fixed. Profiles of temperature along the main flow direction at the burners' level are shown in Fig. 10. As can be seen from Fig. 10, the temperature levels are reduced as A/F increases. As the equivalence ratio decreases the regions of high temperature close to the walls are greatly reduced. Figure 10 shows that the temperature in the furnace central region changes from 1750 to 1700 to 1650 as excess air factor is increased from 1.05 to 1.15 to 1.25. This is expected to influence both heat transfer in one side and the tube burnout at the furnace walls in the other side. The decay in temperature level is much faster at the higher values of excess air factors. The profiles show higher temperature levels in the regions outside the core of the furnace for the case of lower excess air. In the central region, slightly higher temperature values are shown at the high excess air factors. The present results indicate that the excess air factor has negligible effect on the size of the vortex. This is mainly attributed to the fact that the change in air to fuel ratio is achieved through the change in fuel mass flow rate. The volumetric expansions are not significantly affecting the velocity vectors. Figure 11 provides the distributions of NO along the main flow direction for the three cases of excess air factor. The figure indicates a decrease in the highest values of NO as the excess air factor increases. This is attributed to the reduction in the temperature with increase in excess air factor.

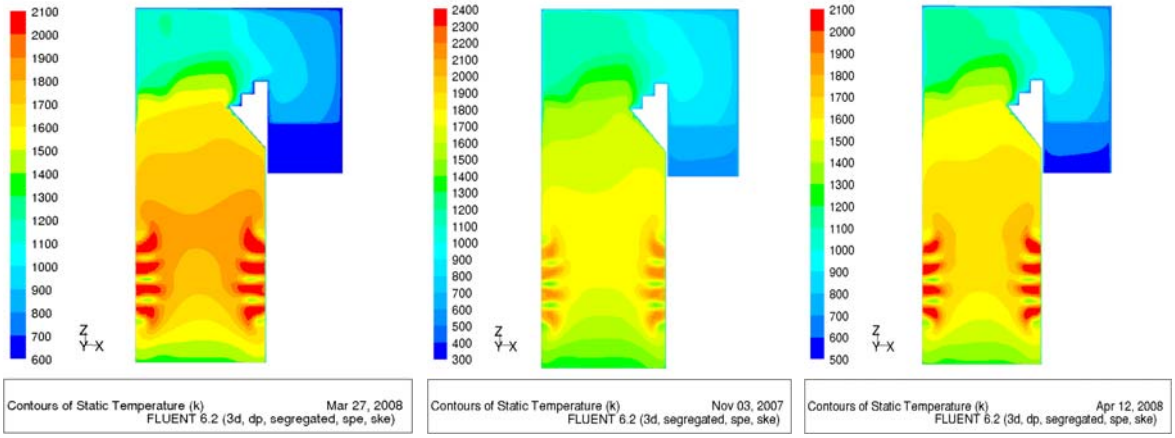

Excess air factor= 1.05 Excess air factor= 1.15 Excess air factor=1.25

Figure 10. Influence of air to fuel ratio on Temperature distribution along an axial section

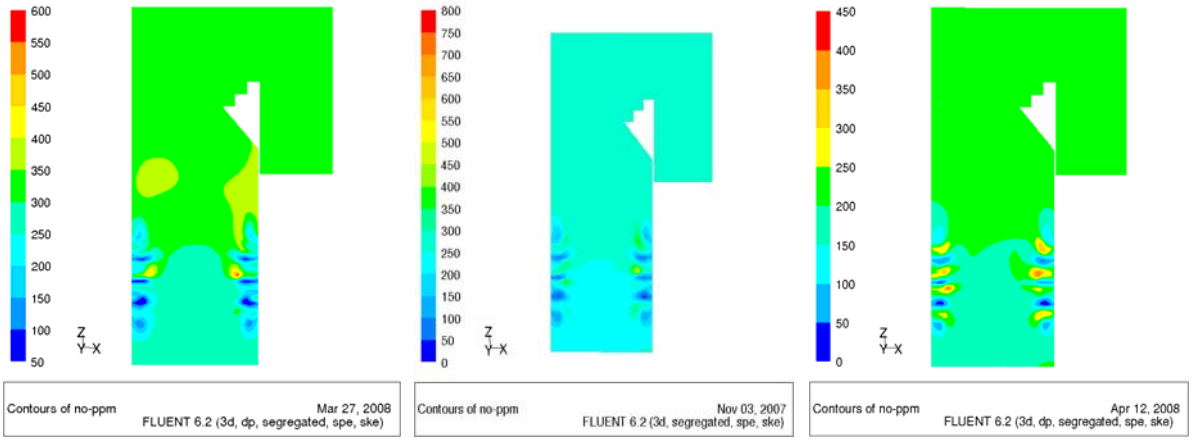

Excess air factor= 1.05 Excess air factor= 1.15 Excess air factor=1.25

Figure 11 Influence of air to fuel ratio on NO distribution along an axial section

The distributions of temperature and NO across the sections of the furnace at the lower and upper burners' levels are shown in Figs. 12 and 14 for temperature and 13 and 15 for NO concentrations. At burner level 1 (lower level), Fig. 12, the effect of the excess air factor is very significant where it is

shown that the regions of high temperature of more than 1650 K are shown in the vicinity of the center at excess air factor of 1.05 while this region is at 1550 K at excess air factor of 1.25. NO distributions are shown in Fig. 13. The figure indicates a considerable decrease in NO values as the excess air is increased. Similar trends are shown in Fig. 14 at the centre of the vortex of the upper level of burners where the temperature changes from 1750 at excess air factor of 1.05 to 1650 at excess air factor of 1.25. NO distributions are shown in Fig. 15. Similar to the distributions at the burners' lower level is the increase in excess air results in reduced values of NO. The results show that two opposing effects exist as a result of decreasing the air-to-fuel ratios. The first is that the expected heat fluxes to the water wall increases, thus, improving the furnace performance. The other effect is that further decrease in the air-to-fuel ratio may result in high wall temperature and consequently tube burnout in real boilers. Thus an optimization of the two effects is required.

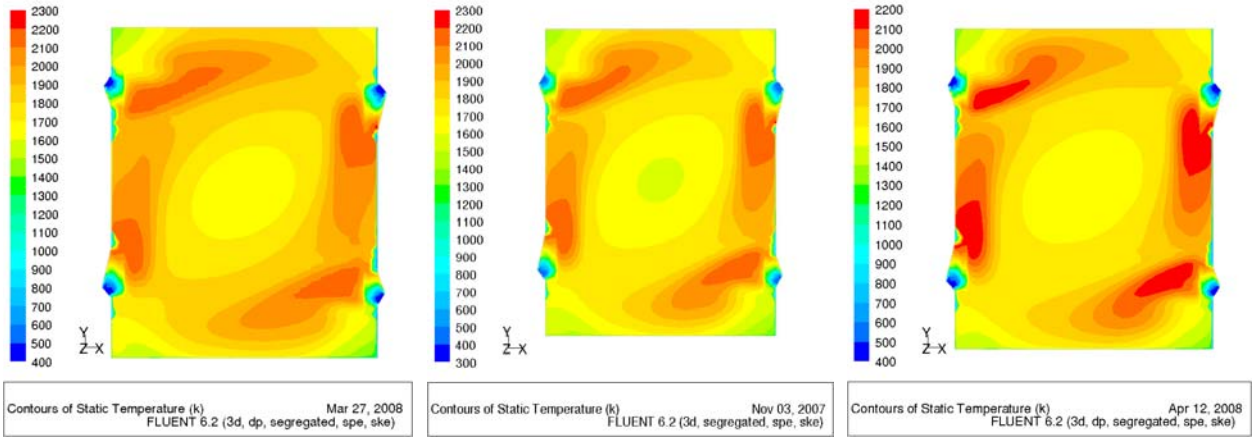

Excess air factor= 1.05 Excess air factor= 1.15 Excess air factor=1.25

Figure 12. Influence of air to fuel ratio on temperature distribution at lower burner level

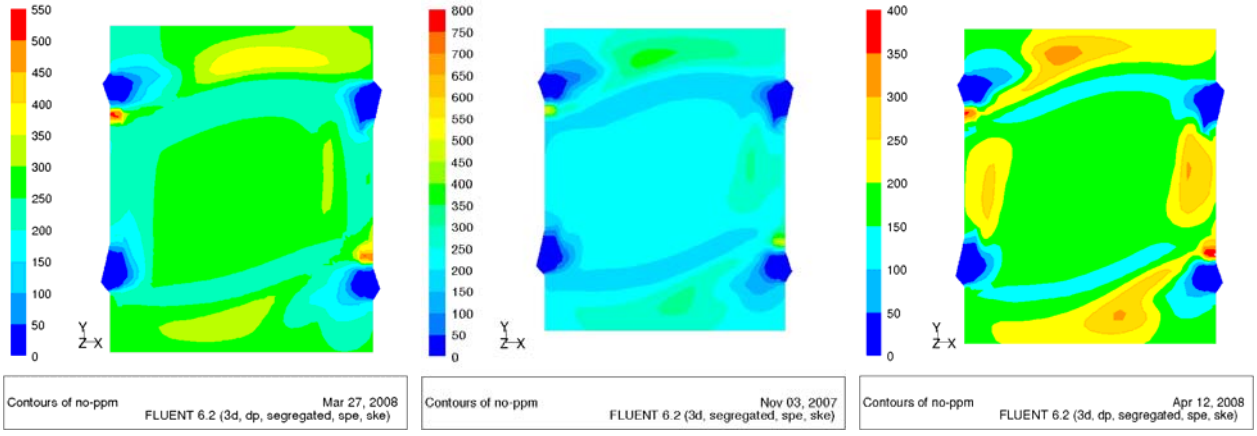

Excess air factor= 1.05 Excess air factor= 1.15 Excess air factor=1.25

Figure 13. Influence of air to fuel ratio on NO distribution at lower burner level

Influence of burner tripping

Four different cases were considered. In the first case (Case I), one burner in the lower level was tripped. In the second case (Case II), two adjacent burners in level 1 were tripped. In case III, two opposite burners were tripped. In the fourth case (case IV), four burners each in one level in the same corner were

tripped. When a burner is tripped, the fuel flow of this burner is cut-off; however, the air remains flowing into the furnace. The fuel flow of the tripped burner is distributed among the other three burners and, thus, the overall air to fuel ratio inside the furnace as well as the total energy input is kept unchanged.

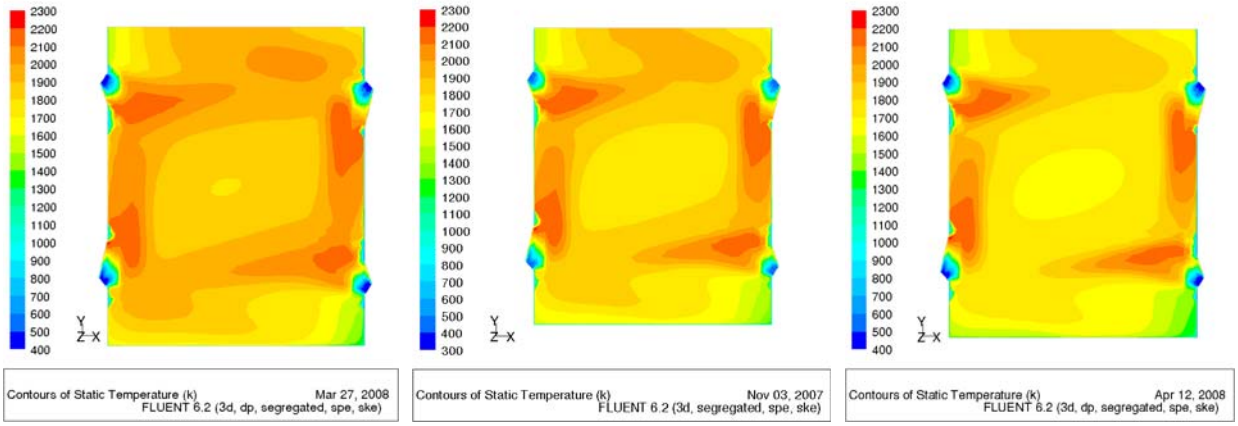

Excess air factor= 1.05 Excess air factor= 1.15 Excess air factor=1.25

Figure 14. Influence of air to fuel ratio on temperature distribution at higher burner level

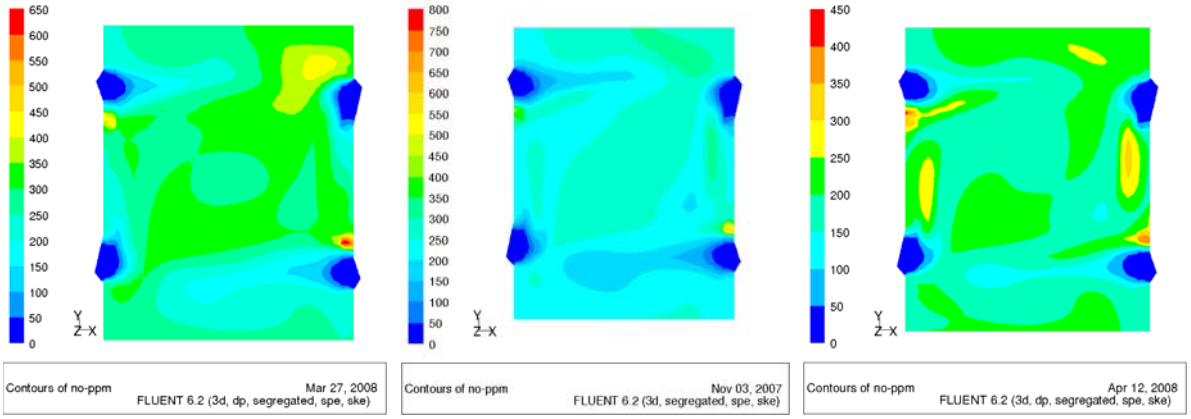

Excess air factor= 1.05 Excess air factor= 1.15 Excess air factor=1.25

Figure 15. Influence of air to fuel ratio on NO distribution at higher burner level

Tripping burners causes destabilization of flames and influences the core vortex. As many burners are tripped, the vortex becomes undefined and the flow field is greatly distorted. The distortion is not due to change in flow momentum as the air flow-rate is unchanged and the fuel flow rate is negligible in comparison to air flow rate. The influence here is due to combustion process and gas volume expansion. The influence of burner tripping is shown in Figs. 16-21. Figure 16 shows the temperature profiles at the middle of the furnace along the flow directions for the four cases of different tripped burners. The distortion of the temperature distribution is shown to be significant as one or two of the burners are tripped. The increase in the wall temperature is clearly indicated in the figure. Tripping two burners reduces temperature in the middle region of the furnace from 1800 for the case of no tripped burners to 1600 for case IV. The contours of temperature for four cases of different tripped number of burners are shown in Figs. 16, 18 and 20. As one of the four burners is tripped, Fig. 18a, the core region is distorted. The region close to the tripped burner is characterized by low temperature values. Due to the fact that the total fuel energy input is same, regions of high temperature appear close to other walls. Regions of high temperature are found close to the walls and near burners. The distortion in temperature distribution may cause destabilization of other burners and in some cases causes their extinguishment. As two adjacent burners (Figs. 18b and 20b) are tripped, it is indicated that the walls are covered with high-temperature

gases. Tripping of two opposite burners (Figs. 18c and 20c) indicates also high temperature at some of the furnace walls. Similar results of temperature distributions are shown for the case of four tripped burners as shown in Fig. 18d and 20d. These results are very significant to the boiler designer due to their influence on tube overheating in these furnace locations.

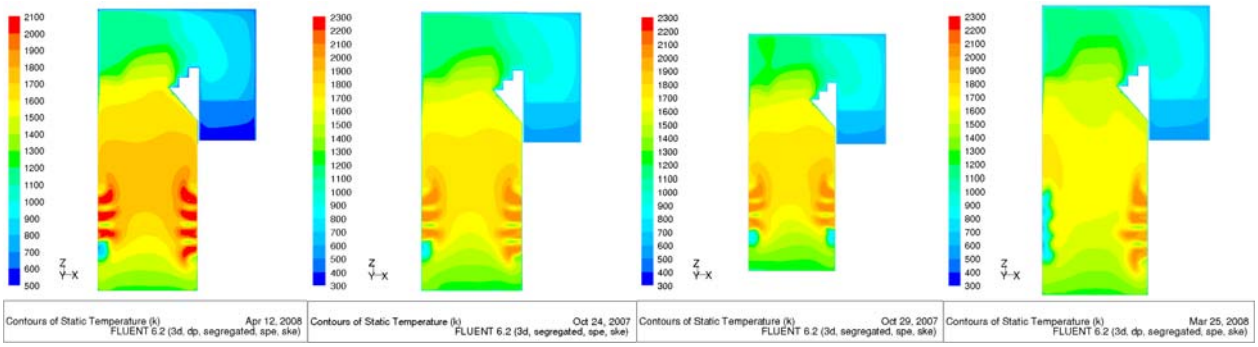

a) Case I b) Case II c) Case III d) Case IV

Figure 16. Influence of burner tripping on temperature distribution along an axial section

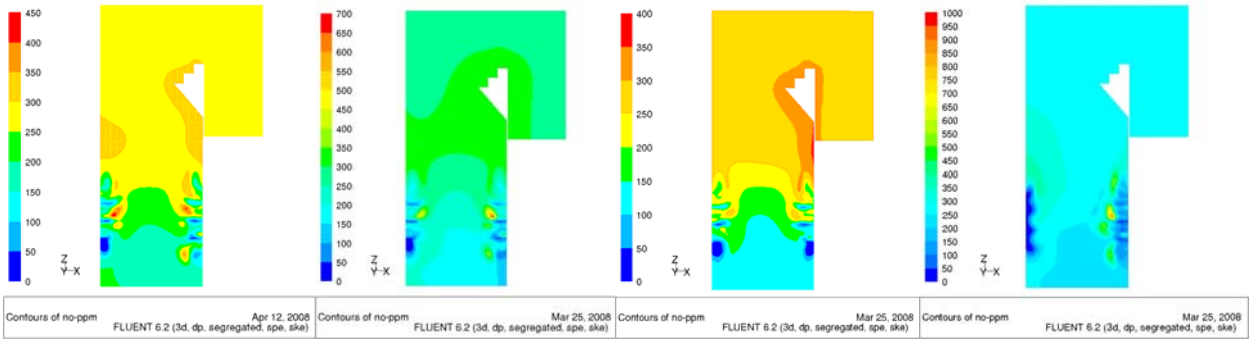

a) Case I b) Case II c) Case III d) Case IV

Figure 17. Influence of burner tripping on NO distribution along an axial section

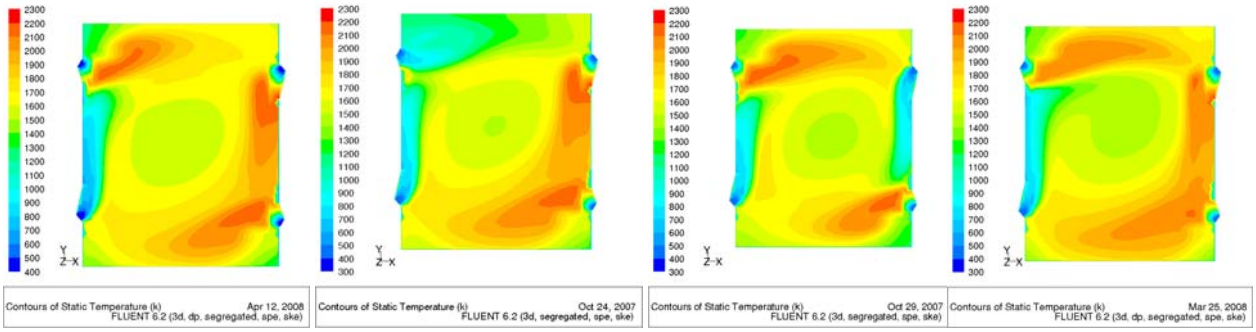

a) Case I b) Case II c) Case III d) Case IV

Figure 18. Influence of burner tripping on temperature distribution at lower level

The NO distributions are shown in Figs. 17, 19 and 21. As can be shown from Fig. 17, small pockets of high NO concentrations appear in each of the four cases. As well, distortion of NO distribution is shown to be significant. Figure 19 provides the NO distributions at the lower level of the burners, level 1. The tripping of one burner results in high distribution of NO where regions of high values of 400 appear

along the axis of two burners with low values at the other burners. Tripping two burners result in more distortion as shown in Fig. 19b and c. Figure 19d shows similar results to those of 19a since the tripping of the burners in the upper levels does not affect the lower level. Investigation of the NO distribution at the upper level of burners show that more distortion in NO production in comparison to those of Fig. 19 (lower level, 1). Regions of high values of NO appear as the number of tripped burners (in the same level) increase.

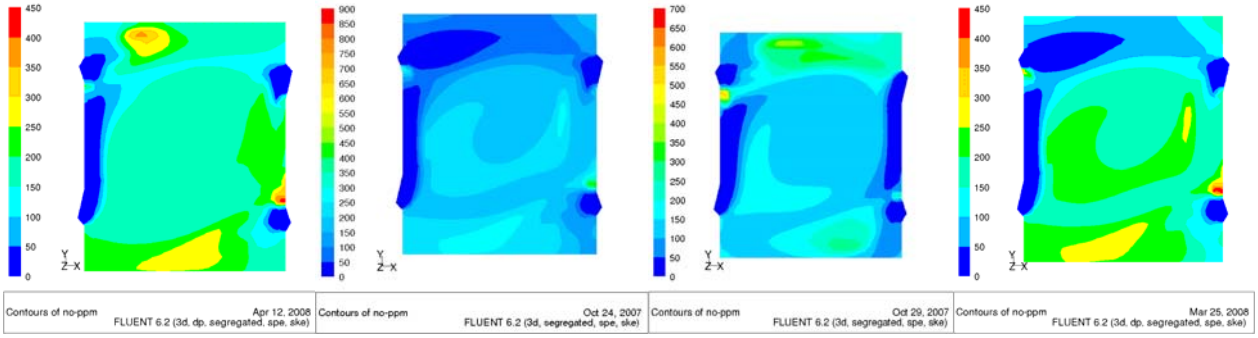

a) Case I b) Case II c) Case III d) Case IV

Figure 19. Influence of burner tripping on NO distribution at lower level

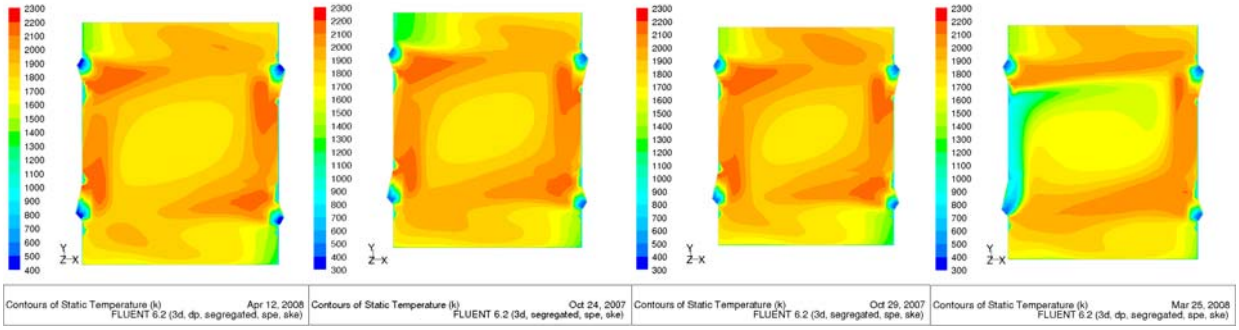

Case I Case II Case III Case IV

Figure 20. Influence of burner tripping on temperature distribution at higher level

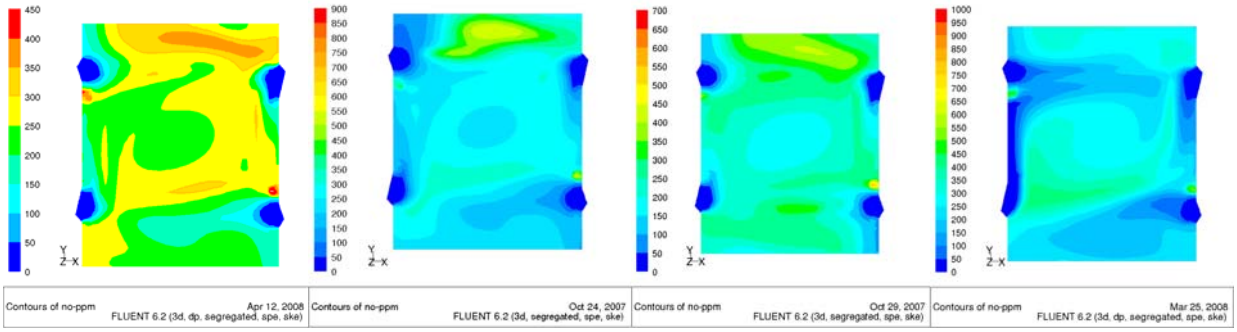

Case I Case II Case III Case IV

Figure 21. Influence of burner tripping on NO distribution at higher level

Correlations

In order to analyze the influence of the different parameters on NO characteristics, the global characteristics of the whole furnace are considered. Here, representative values of maximum, average and outlet of furnace for NO and temperature are considered for the analysis. Correlations for NO with the main parameters are presented. The NO maximum value and the value at the outlet section are

polynomially functions of the combustion air temperature as given by equations 22 and 23. NO is in ppm and temperature is in K. The influence of the excess air factor λ on the maximum value and the value at the outlet section are given in equations 24 and 25.

$$NO, out = 0.0042 (T_{air})^2 - 2.23 T_{air} + 483.4 \quad (22)$$

$$NO, max = 0.047(T_{air})^2 - 39.8 T_{air} + 9177.8 \quad (23)$$

$$NO, max = -7346.4 (\lambda)^2 + 16092 \lambda - 8005.7 \quad (24)$$

$$NO, out = -532.53(\lambda)^2 + 674.82 \lambda + 194.55 \quad (25)$$

The average value of NO at the outlet section as well as the maximum NO value are proportionally increased with the square of the combustion air temperature. On the other hand, the average value of NO at the outlet section as well as the maximum NO value are proportionally reduced with the square of the combustion air temperature.

Figure 22 presents the influence of the combustion air temperature on the NO at the furnace outlet section and the maximum value. The figure shows that the outlet NO value increase from 270 to 670 ppm as the temperature increases from, 400 to 600 K. However, the maximum value increases to more than three times as T_{air} increases from 400 K to 600 K. The influence of excess air factor on NO distributions is shown in Fig. 23 for maximum NO values and at the outlet section. As excess air factor increases, NO values decrease from 320 ppm to 200 ppm. The maximum value also decreases from 800 ppm to 600 ppm.

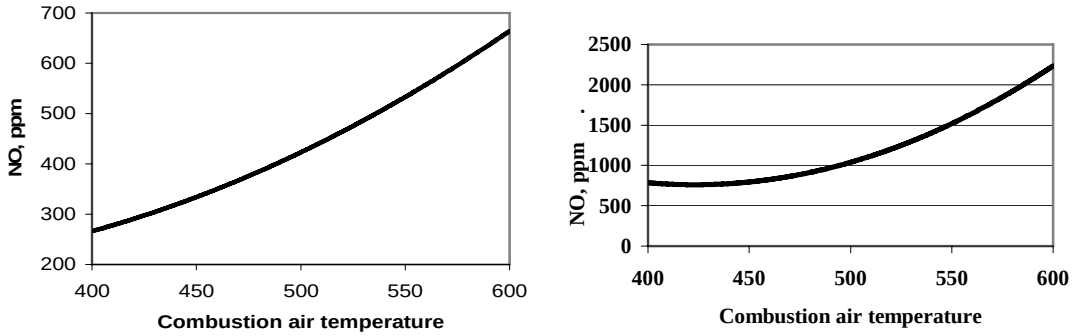

a) NO concentration at outlet section **b)** NO concentration (maximum values)

Figure 22 Influence of combustion air temperature on NO concentration

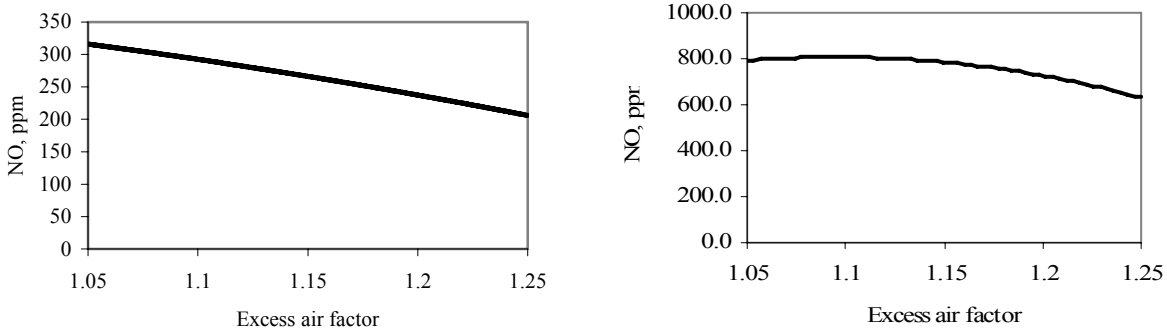

a) NO at outlet section **b)** Maximum NO concentration

Figure 23 Influence of excess air factor on NO concentration

Conclusions

The influence of the combustion air temperature, fuel to air ratio and burner tripping on the thermal fields and NO distributions are presented. The results indicate a vortex having reduced temperature levels at the middle of the furnace cross section as a result of the adverse pressure gradient. Available experimental measurements were used for validating the calculation procedure. The results show that combustion air temperature greatly influences the NO formation. NO formation is mainly correlated to the maximum and average furnace temperature. As the combustion air temperature increases, furnace temperature increases and the thermal NO concentration increases sharply. The results have shown that the furnace average temperature and NO concentration decrease as the excess air factor increases for a given air mass flow rate. The results show that tripping one or two burners either adjacent or opposite or tripping four results in regions of high temperature gases close to the walls. The results show that the temperature and NO distributions are significantly distorted by tripping any of the burners.

Nomenclature

A/F	air-to-fuel ratio on a mass basis
C_1	constant (Eq. 6)
C_2, C_3	constant (Eq. 8)
C_μ	constant (Eq. 4)
G	generation of kinetic energy of turbulence
I	total radiation intensity
J	diffusion flux of species
k	kinetic energy of turbulence
m_i	mass of species
P	pressure
$\dot{Q}$	Rate of heat absorption
R	mass rate of reaction
T	temperature
S	source term
$\overline{U}$	Mean velocity
u	fluctuating velocity component
Y	species concentration

Superscripts

—	time average

Greek letters

ε	dissipation rate of turbulent kinetic energy
μ	dynamic viscosity
κ	absorption coefficient
λ	wavelength
Φ	dependent variable
ϕ	fluctuation in the dependent variable Φ
ρ	average density
σ_k	effective Prandtl number for k
σ_ε	effective Prandtl number for ε
Θ	angle of burner inclination

Subscripts

air	combustion air
avg	average value
econ	economizer
b	blackbody
eff	effective
k	turbulent kinetic energy
λ	excess air factor
max	Maximum value
NO	nitrogen oxide
out	outlet section
Φ	dependent variable
sup	superheater

Acknowledgment: *The Authors would like also the Acknowledge the support of King Fahd University of Petroleum and Minerals during all the phases of this project.*

References

Afonso R, Dusatko GC, Pohl JH, (1993) Measurements of NOx emission from coal boilers, *Combustion Science and Technology*, **93**, 41–51.

Attya AM, Habib MA, (1990) The Influence of Spray Characteristics and Air Preheat on the Flame Properties in a Gas Turbine Combustor, Multi-phase Transport and Particulate Phenomena, Ed. T. Nejat Veziroglu, Hemisphere Publishing Corporation, N. Y., Vol. 3, pp. 543-566.

Backreedy RI., Jones JM, Ma L, Pourkashanian M, Williams A, Arenillas A, Arias B, Pis JJ, Rubiear F, (2005) Prediction of unburned carbon and NOx in a tangentially fired power station using single coals and blends. *Fuel*, **84**, 2169-2203.

Boyd RK, Roscarel KJ, Kent JH, (1985) Gas Flow and Mixing in a Tangentially Fired Furnace, *Third Australasian Conference on Heat & Mass Transfer*, St. Leonards, May 13-15, pp. 51-58

Chen JY, Mann AP, Kent JH, (1992) Computational Modeling of Pulverized Fuel Burnout in Tangentially *Fired Furnaces, Symposium (International) on Combustion, Combustion Inst*, Pittsburg, PA, USA. pp 1381-1389

Chong AZS, Wilcox SJ, Ward J, (2001) Prediction of gaseous emissions from a chain grate stoker boiler using neural networks of ARX structure. IEE Proc. *Sci. Meas. Technol*., **148**, 95-102.

Coelho PJ, Carvalho MG, (1995) Mathematical Modeling of NO Formation in a Power Station Boiler, *Combustion Sci. and Tech*., **108**, 363-382.

Coelho PJ, Carvalho MG, (1996) Evaluation of a Three-Dimensional Mathematical Model of a Power Station Boiler. *Journal for Gas Turbines and Power*, **118**, 887-895.

Dong W, (2000) *Design of advanced industrial furnaces using numerical modelling method*, Ph.D. Thesis, Department: Department of Materials Science and Engineering, Stockholm, ISBN: 91-7170-500-7.

Fan JR, Sun P, Zheng YQ, Ma YL, Cen K F, (1999) Numerical and experimental investigation on the reduction of NOx emission in a 600 MW utility furnace by using OFA, *Fuel*, **78**, 1387–94.

Fan JR, Zha XD, Cen KF, (2001a) Study on Coal Combustion Characteristics in a W-Shaped Boiler Furnace, *Fuel*, **80**, 373-381.

Fan, J., Qian, L., Ma, Y., Sun, P. and Cen, K., 2001b, Computational modeling of pulverized coal combustion processes in tangentially fired furnaces, Chem. Eng. J., Vol. 81 (1–3), pp. 261–269.

Fluent 6.2 User's Guide, (2003) Fluent Inc., Center Research Park, 10 Cavendish Court, Lebanon, NH 03766, USA.

Frassoldati A, Firgerio S, Colombo E, Inzoli F, Faravelli T, (2005) Determination of NO_x Emissions from Strong Swirling Confined Flames with an Integrated CFD-based Procedure, *Chemical Engineering Science*, **11**, 2851-2869.

Habib MA, Ben-Mansour R, Antar MA, (2005) Flow Field and Thermal Characteristics in a Model of a Tangentially Fired Furnace under Different Conditions of Burner Tripping, *Journal of Heat and Mass Transfer*, **41**, 909-920.

Habib MA, El-Mahallawy FM, Abdel-Hafez A, Nasseef N, (1992) Stability Limits and Temperature Measurements in a Tangentially-Fired Model Furnace, *Energy*, **17,** 283-294.

Habib MA, Whitelaw JH, (1982) The Calculation of Turbulent flow in wide angle diffusers, *Num. Heat Transfer*, **5,** 145-164.

Habib MA, Attya AE, McEligot DM, (1989) Calculation of turbulent flow and heat transfer in channels with stream wise periodic flow, *ASME Journal of Turbomachinery*, **110**, 405-411

Handby VI, Li G, (1997) Modelling of Thermal Emissions Performance of Commercial Boilers, *Int. Journal of Heating, Ventilating, Air-Conditioning and Refrigerating Research*, **3**, 101-111.

Hanson RK, Salimian S, (1984) Survey of Rate Constants in H/N/O Systems, In W. C. Gardiner, Ed., *Combustion Chemistry*, p. 361.

He B, Chen M, Yu Q, Liu S, Fan L, Sun S, Xu J, Pan WP, (2004) Numerical study of the optimum counter-flow mode of air jets in a large utility furnace, *Comput. Fluids*, **33**, 1201-1223.

He B, Zhu L, Wang J, Liu S, Liu B, Cui Yi, Wang L, Wei G, (2007) Computational fluid dynamics based retrofits to reheater panel overheating of No. 3 boiler of Dagang Power Plant, *Computers & Fluids*, **36**, 435-444.

Hjertager LK, Hjertager BH, Solberg T, (2001) *CFD Modelling of Fast Chemical Reactions in Turbulent Liquid Flows,* Chemical Engineering Laboratory, Aalborg University Esbjerg, Niels Bohrs vej 8, DK-6700 Esbjerg, Denmark.

Hjertager LK, Osenbroch J, Hjertager BH, Solberg T, (2000) Validation of the Eddy Dissipation Concept for fast chemical reactions in turbulent flows, *Chemical Reaction Engineering* VII: CFD, 6-11 August, Quebec City, Canada.

Kokkinos A, Wasyluk D, Adams D, Yavorsky R, Brower M, (2001) B & W [s] Experience Reducing NO_x Emissions in Tangentially-fired Boilers, The U.S. EPA/DOE/EPRI Combined Power Plant Air Pollutant Control Symposium; *The Mega Symposium*, Aug. 20-23, Chicago, Illinois, U.S. A.

Kokkinos A, Wasyluk D, Brower M, Berna JJ, (2000) Reducing NO_x Emissions in Tangentially-fired Boilers- A new Appraoch, ASME *International Joint Power Generation Conference*, July 24-25, Miami, Florida, U.S.A.

Launder BE, Spalding DB, (1974) The numerical computation of turbulent flows, *Computer Methods in Applied Mechanics and Engineering,* **3**, 269-289.

Li G, (1997) Modelling of Thermal and Emission Performance of Commercial Boiler, International *Journal of Heating, Ventilation, Air Conditioning, and Refrigeration Research*, **3**, 101-111.

Li K, Thompson S, (1996) A cascaded neural network and its application to modeling power plant pollutant emission, *Proceedings of the 3rd World Congress on Intelligent Control and Automation*.

Li N, Thompson S, (1996) A Simplified Non-Linear Model of NOx Emissions in a power Station Boiler, *UKACC International Conference on Control* '96, 2-5 September, No. 427, 1016-1021.

Liierup JB, Dam-Johansen K, Glarborg P, (1994) Characterization of a full-scale, single-burner pulverizedcoal boiler: temperatures, gas concentrations andnitrogen oxides. *Fuel*, **73**, 492–499.

Liu F, Becker, HA, Bindar Y, (1998) A Comparative Study of Radiative Heat Transfer Modeling in Gas-Fired Furnaces Using the Simple Grey and the Weighted-Sum-of-Grey-Gases Models. International *J. of Heat and Mass Transfer*, **41**, 3357-3371

Liu XJ, Xu XC, Fan HL, (2001) Further studies on the coal combustion behavior in the tangentially fired boiler furnace, *Proceedings of the Chinese Society of Electrical Engineering*, **21**, 80-84.

Lou C, Zhou HC, (2005) Deduction of the two-dimensional distribution of temperature in a cross section of a boiler furnace from images of flame radiation *Combustion and Flame*, **143**, 97–105

Luis I. Dı´ez,L. I., Corte´s, C. and Campo, A., 2005, Modelling of pulverized coal boilers: review and validation of on-line simulation techniques, *Applied Thermal Engineering* **25**, 1516–1533

Ma CY, Mahmoud T, Gaskell PH, Hampertsoumian E, (1999) Numerical Predictions of a turbulent diffusion flame in a cylindrical combustor using eddy dissipation flamelet combustion models, *Proc. Instn. Mech. Engrs*., **213(C)**, 697-705.

Magnussen BF, Hjertager BH, (1976) On mathematical models of turbulent combustion with special emphasis on soot formation and combustion, In *16th Symp. (Int'l.) on Combustion,* The Combustion Institute, 1976.

Mathur MP, Gera D, Freeman M, (2001) Computational Fluid Dynamics Modeling Analysis of Combustors, 2001 Joint AFRC/JFRC/IEA, *Combustion Symposium, Kauai*, HI, September 9-12.

Modak AT, (1979) Radiation from products of combustion, *Fire Research*, **1**, 339-3361.

Patankar SV, (1980) *Numerical Heat Transfer and Fluid Flow*, First Edition, Taylor and Francis.

Raithby GD, Chui EH, (1990) A Finite-Volume Method for Predicting a Radiant Heat Transfer in Enclosures with Participating Media, *J. Heat Transfer*, **112**, 415-423.

Reynolds WC, (1987) *Fundamentals of turbulence for turbulence modelling and simulation*, Lecture Notes for Von Karman Institute, Agard Report No. 755.

Robinson GF, (1985) A Three-Dimensional Analytical Model of a Large Tangentially Fired Furnace, *J. Institute of Energy* **58**, 116-150.

Shih TH, Liou WW, Shabbir A, Zhu J, (1995) A new k-ε eddy-viscosity model for high Reynolds number turbulent flows - Model development and validation, *Computers and Fluids,* **24**, 227-238.

Shuja SZ, Habib MA, (1996) Fluid Flow and Heat Transfer Characteristics in Axisymmetric Annular Diffusers, *Computers and Fluids*, **25**, 133-150.

Smith TF, Shen ZF, Friedman JN, (1982) Evaluation of Coefficients for the Weighted Sum of Gray Gases Model, *J. Heat Transfer*, **104**, 602-608.

Thou YG, Zhang MC, Xu TM, Hui SF (2001) Experimental and numerical study on the flue gas velocity deviation in a tangentially fired boiler furnace, *Proceedings of the Chinese Society of Electrical Engineering*, **21**, 68-72.

Van der Lans RP, Glarborg P, Dam-Johansen K, Knudsen P, Hesselmann G, Hepburn P., 1998, Influence of coal quality on combustion performance. *Fuel*, **77**, 1317-1328.

Versteeg HK, Malalasekera W, (1995), *An Introduction to Computational Fluid Dynamics; the Finite Volume Method*, Longman Scientific and Technical.

Walsh PM, Xie JY, Douglas RE, Battista JJ, Zawadzki EA, (1994) Unburned carbon loss from pulverized coal combustors. *Fuel,* **73,** 1074-1081.

Wilcox DC, (2000) *Turbulence Modelling for CFD*, DCW Industries.

Xiang J, Sun XX, Hu S, Yu DX, (2000) An experimental research on boiler combustion performance. *Fuel Processing Technology*, **68**, 139–151.

Xu MH, Azevedo JLT, Carvalho MG, (2001) Modelling of the combustion process and NOx emission in a utility boiler. *Fuel,* **79**, 1611-1619.

Yaga M, Sasada K, Yamamoto T, Aoki H, Miura T, (2000) An Eddy Characteristic Time Modeling In Les For Gas Turbine Combustor Mitsuru, Proceedings of 2000 *International Joint Power Generation Conference Miami Beach,* Florida, July 23-26, pp. 1-6.

Yin C, Caillat S, Harion JC, Baudoin B, Perez E, (2002) Investigation of the Flow, Combustion, Heat Transfer and Emissions from a 609 MW Utility Tangentially Fired, Pulverized Coal Boiler, *Fue*l, **81**, 997-1006.

Zheng Y, Fan J, Ma Y, Sun, P, Cen K, (2000) Computational modelling of Tangentially Fired Boiler II NO_x Emissions, *Chinese J. of Chemical Engineering*, **8**, 247-250.

Zhou H, Cen K, Fan J, (2004) Modelling and optimization of the NOx emission characteristics of a tangentially fired boiler with artificial neural networks, *Energy*, **29**, 167-183.

Zhou Y, Dou Y, Jiang H, Hui S, Xu T, (1999) Effect of furnace structure on velocity deviation tangentially fired boiler, *J. of Xi'an Jiaotong University,* **33**, 32-35.